Journal of Brilliant Engineering 4 (2026) 41143

Brilliant Engineering

journal home: www.acapublishing.com/journals/4/ben

Research Article

Comparison of Abrasion Resistance and Surface Roughness of Foundry Patterns Produced from GG25 and GGG50 Grade Cast Iron

Ali Zeynalli[1], Derya Tekin*,[2]

[1,2]*Department of Metallurgy and Materials Engineering, Atatürk University, Erzurum, Türkiye*

Keywords

Gray cast iron,
Wear behavior,
Ductile cast iron,
Pattern material,
Green sand patterning.

Abstract

Pattern materials used in green sand patterning lines are continuously exposed to abrasive sand particles and repetitive mechanical loads, which can affect their dimensional stability and service life. In this study, the dimensional wear behavior of GG25 gray cast iron and GGG50 ductile cast iron pattern materials was investigated under industrial green sand patterning line conditions. Wear performance was evaluated using weight loss and dimensional changes after 16,794 patterning cycles, while surface roughness was assessed only for the initial machined condition. The results showed that both materials exhibited relatively similar dimensional wear behavior under the conditions studied. However, GG25 cast iron was observed to exhibit a lower measured mass loss and a relatively smoother surface texture. These observations suggest that material-dependent differences may affect wear performance during operation. Surface roughness was measured before patterning to characterize the initial machined surface finish. Furthermore, due to the limited number of cycles, variations in sample geometry, and the absence of repeated samples and direct microstructural characterization, the results should be interpreted cautiously. The findings provide a preliminary insight into the dimensional wear behavior of cast iron pattern materials under real industrial operating conditions and may form a basis for future studies involving larger sample sizes and more comprehensive material characterization.

1. Introduction

Cast irons are iron-carbon alloys with a higher carbon content than conventional carbon steels. In addition, cast iron materials contain silicon additives that support a better casting process due to the graphite particles present in the matrix. Examples of these silicon additives include malleable and ductile irons, as well as white and gray cast iron [1-4]. Ductile iron (DI-GGG50) is a well-known iron alloy composed of Fe, Si, and C. Due to its moderate wear and fatigue resistance, good machinability, and high forgeability, DIs-GGG50 has a very wide range of applications in valves, crankshafts, pumps, railway systems, wind turbines, heavy-duty engine parts, and pistons. However, the low wear resistance of cast iron is a disadvantage. Therefore, various additive processes are carried out to improve the wear performance of ductile iron and increase its surface hardness [5, 6]. Compared to steels, DI-GGG50 has lower densities (10%) and lower production costs. Consequently, their lower density, reduced production costs, and comparable mechanical quality make ductile irons superior candidates compared to steel. On the other hand, DI-GGG50 can exhibit the best combination of mechanical properties, such as fracture toughness, strength, and ductility, among other white and gray cast irons. The matrix of DIs can be pearlitic, ferritic, or a combination of pearlitic and ferritic. The type of matrix plays a role in determining the mechanical properties. Another type of cast iron, grey cast iron (GCI-GG25), is widely used in the production of some machine parts. Specific cooling rates are applied to GG25 gray cast iron during solidification to optimize its microstructural and surface properties. Cast irons find wide application in industry because they offer high machinability in terms of power consumption, good castability, cutting forces, strength-to-cost ratio, and tool wear. The damping capacity of GCI-GG25 makes it suitable for machine tool bases and frames, measuring equipment, and engine blocks. In a 2009 survey conducted by Modern Casting, grey cast iron was the most commonly used cast metal among 34 countries [7]. Graphite flakes formed during the solidification process help control mechanical properties and contribute to the toughness and low-strength characteristics of gray cast iron. The microstructure of gray cast iron is characterized by graphite lamellae dispersed within the iron matrix. The amount of graphite, as well as the distribution, morphology, and size of the graphite lamellae, play a role in determining mechanical behavior. Gray cast iron, which has a higher damping capacity compared to steel and other types of cast iron, is thought to owe this property to its flake graphite structure [5, 8].

In green sand patterning processes, metal patterns are generally preferred to meet mass production requirements. The pattern material affects not only the production cost but also the dimensional accuracy, surface quality, and overall efficiency of the patterning line. Incorrectly prepared pre-cut material or inadequate surface treatment processes can prevent the patterns from being removed from the sand, leading to pattern breakage and causing machining errors and raw material waste in the final casting [9, 10]. Although numerous studies in the literature have focused on the mechanical properties of cast irons, field-based investigations comparing the wear behaviour and initial machined surface quality of different cast iron grades, particularly lamellar graphite GG25 and spheroidal graphite GGG50, under real production line conditions remain limited [11]. Considering that metal patterns are generally expected to withstand up to approximately 100,000 patterning cycles, progressive wear and dimensional deviation over time pose a significant risk to production quality [11, 12].

This study aims to experimentally investigate the wear resistance and initial machined surface quality of patterns manufactured from GG25 and GGG50 grade cast irons in an actual green sand patterning line. By conducting the experiments in an active industrial environment rather than a laboratory setting, this research investigates performance differences between the two materials under industrial conditions.

*Corresponding Author: deryatekin@atauni.edu.tr
Received 28 Apr 2026; Revised 23 Jul 2026; Accepted 27 Jul 2026
https://doi.org/10.36937/ben.2026.41143

2. Materials and Method

2.1. Materials

In this study, two different cast iron grades commonly used as pattern materials in foundry applications were investigated: GG25 gray cast iron and GGG50 ductile cast iron. Both materials were cast from the same pattern to eliminate variations arising from casting geometry and solidification conditions. The chemical compositions and material grades were selected in accordance with relevant standards for gray and ductile cast irons. Billets produced from each material were machined using an identical CNC machining program to obtain patterns with the same geometry and dimensional tolerances. By keeping the pattern design and machining parameters constant, the influence of material type on surface roughness and wear behaviour was isolated [13].

2.2. Pattern preparation and machining

The patterns were designed using CAD software and manufactured under identical machining conditions. All machining operations were performed using the same cutting strategy and tool path parameters to ensure comparable surface conditions after machining [14, 15]. No additional surface treatments or coatings were applied to the patterns. After machining, the initial dimensions and weights of both patterns were recorded to establish baseline reference values for subsequent wear measurements.

2.3. Green sand patterning process

The prepared patterns were installed simultaneously on an automatic green sand patterning line operating under industrial production conditions [16, 17]. Both patterns were subjected to the same pattering parameters, including sand system, compaction method, and cycle time. Wear measurements were conducted after predefined pattering intervals. Dimensional and weight measurements were performed after 4,158, 9,828, and 16,794 pattering cycles to evaluate the progressive wear behaviour of each pattern material.

2.4. Surface roughness measurements

Surface roughness measurements were carried out immediately after machining using a portable contact-type profilometer. Due to the limited measurement area on the pattern surfaces, a custom fixture was used to ensure stable positioning of the device during measurements [18]. Multiple measurements were taken at selected locations on each pattern surface, and the average roughness (Ra) values were calculated. All profilometer settings were kept at the manufacturer's default parameters to ensure measurement consistency. Based on ISO 8062-3, which defines general dimensional and geometrical tolerances for castings, the machining tolerance was determined as ±0.2 mm.

2.5. Wear evaluation

Pattern wear was evaluated based on changes in weight and critical dimensions over the pattering cycles. Weight measurements were performed using a high-precision digital balance with a resolution of 0.01 g, while dimensional measurements were carried out using a digital caliper with 0.01 mm resolution. The recorded changes were used to compare the wear resistance of GG25 and GGG50 pattern materials under real production conditions [19].

2.6. Brinell hardness test

The hardness of GG25 grey cast iron and GGG50 ductile cast iron pattering materials was evaluated using the Brinell hardness test. Before testing, the sample surfaces were sanded and cleaned to remove any contaminants and ensure a smooth and even test surface. Measurements were performed using a Brinell hardness tester with 10 mm diameter tungsten carbide ball tips (HBW). The hardness values of the samples were measured before pattering. The hardness of the cast irons was measured under a load of 3000 kgf (29.42 kN) for 10-15 seconds. Three indentations were created at different points on each sample, and the diameter of each indentation was automatically measured by the hardness tester, and the corresponding Brinell hardness values were calculated. Finally, the standard deviation was calculated to assess the repeatability of the measurement.

2.7. Optical microscope examination of GG25 and GGG50 cast irons

Before microstructural analysis, cast irons were treated to remove surface impurities using silicon carbide (SiC) abrasives of 600, 800, 1000, and 1200 grit. The surfaces were then polished using diamond suspensions to achieve a mirror-like finish. To examine the phases in the composition of the polished surfaces, samples were etched in a 2% Nital solution for 15 seconds. Finally, they were examined under an optical microscope at 100X magnification.

3. Results and Discussion

Surface roughness results obtained from Ra measurements taken from three different regions of the sample surface for each pattern material are given in Table 1. The first three measurements correspond to the GGG50 specimen, while the subsequent three correspond to the GG25 specimen. The arithmetic mean of the measured values was considered the representative surface roughness for each specimen, ensuring reliable comparison between the pattern materials.

Table 1. Ra measurements for each pattern material

Measurement No	Ra	Ixn
1 (GGG50)	1.47791	5 x 0.8
2 (GGG50)	1.46859	5 x 0.8
3 (GGG50)	1.44337	5 x 0.8
4 (GG25)	1.07984	5 x 0.8
5 (GG25)	1.02163	5 x 0.8
6 (GG25)	0.960641	5 x 0.8

For the GGG50 specimen, the measured Ra values ranged from 1.443 to 1.478 µm, yielding an average surface roughness of 1.4633 µm. The narrow variation range indicates a relatively uniform surface condition after machining. In contrast, the GG25 specimen exhibited Ra values between 0.960 and 1.079 µm, with an average surface roughness of 1.0207 µm.

Based on the results from specific industrial trials, the GG25 pattern showed a lower initial machined Ra value and a lower measured mass loss value, while dimensional losses were generally similar. This difference may be attributed to differences in the machining response of the two cast iron grades. Gray cast iron is often reported to produce smoother machined surfaces due to its characteristic graphite morphology, which can facilitate chip formation during cutting. However, it should be noted that the present measurements were performed only on the machined patterns prior to patterning operations. Therefore, the results provide information on the initial surface quality of the patterns and do not allow conclusions to be drawn regarding surface roughness evolution or surface stability during repeated green sand patterning cycles. Table 2 shows the chemical composition values for GG25 and GGG50 cast iron. The cast iron materials given in Table 2 were commercially produced by the supplier according to EN 1561 (GG25) and EN 1563 (GGG50) standards, and the reported chemical compositions were provided by the manufacturer.

Table 2. Chemical compositions of the tested GG25 and GGG50 cast iron materials

Element	GG25 Weight (%)	GGG50 Weight (%)
Fe	93.4	93.0
C	3.22	3.62
Si	2.11	2.44
Mn	0.657	0.332
P	0.0399	0.0373
S	0.0965	0.0152
Cr	0.0262	0.0286
Mo	<0.0020	0.0028
Ni	0.0173	0.0136
Co	0.0031	0.0036
Cu	0.369	0.345
Ti	0.0201	0.0253
V	0.0040	0.0063
Pb	0.0031	<0.0025
Zr	0.0030	0.0052
Mg	<0.01%	0.0429

After the completion of the pattern manufacturing process and prior to installation on the patterning plate, an initial dimensional and weight measurement was carried out to establish reference values for subsequent wear evaluations. The primary purpose of this initial measurement was to verify the conformity of the machined patterns with the CAD design and technical drawings, as well as to provide accurate baseline data for calculating dimensional deviations during the patterning process. Four critical dimensions were selected for monitoring: two diameters measured beneath the corner radius (38.27 mm and 59 mm) and two height dimensions (50 mm and 10 mm). To minimize measurement uncertainty, each dimension was measured three times, and the average value was recorded. Table 3 shows the Nominal Operating Ranges of the sand used after 5 measurements taken at different time intervals. Figure 1 shows the technical drawing of the test specimen.

Table 3. Nominal Operating Ranges of Green Sand After 5 Measurements

Sand characteristics	Measurement-1	Measurement-2	Measurement-3	Measurement-4	Measurement-5
Gas Permeability	108	98	100	100	103
Compactibility %	47.96	44.67	46.2	46.05	47.16
Moisture content %	3.81	3.81	3.80	3.76	3.80
Mass loss of ignition				5	
Compressive Strength	10.2	11	11.1	12.1	12.2
Shear Strength N/sn^2	2.3	2.7	2.3	2.4	2

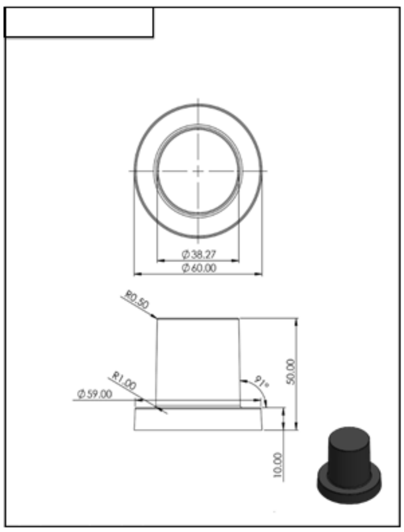

Figure 1. Technical drawing of the test sample

Initial measurements show that all dimensions of both the GG25 and GGG50 dies are within the specified machining tolerances. The maximum initial deviation was measured as 0.08 mm, while the minimum deviation was only 0.01 mm, indicating high dimensional accuracy after machining. Because the mounting hole geometry is different, the mass loss data was also normalized according to the exposed surface area and carefully interpreted. The mounting holes drilled on the bottom of the sample are where the sample is attached to the plate. No measurements are taken from these areas, nor is there any contact with sand. Therefore, direct abrasive contributions are expected to be limited, but their effects cannot be entirely ruled out.

Since these holes were not identical in size and number, part of the initial weight difference may be related to geometric variation rather than intrinsic material properties. Considering the density difference between GG25 and GGG50, a small weight variation may also arise from material-related factors; however, under practical casting conditions, this difference is expected to be limited. Because the mounting holes were located on the bottom surface, which remained in contact with the patterning plate during operation, direct exposure to abrasive sand was considered minimal. Therefore, although the influence of hole geometry on weight-loss measurements cannot be completely excluded, differences in mounting hole depth are expected to have only a limited influence on the wear evaluation. After four weeks of production corresponding to 4,158 pattering cycles, the second-dimensional inspection was conducted. At this stage, the GGG50 pattern exhibited its greatest dimensional change at the 50 mm height (H-50), with a reduction of 0.11 mm, while the smallest change was observed at the 10 mm height (H-10) with only 0.02 mm. Similarly, the GG25 pattern showed the most pronounced dimensional reduction at the 50 mm height, whereas no measurable change was detected at the 10 mm height. These results indicate that height-related dimensions were more sensitive to early-stage wear, likely due to repeated contact and stripping forces acting in the pattern opening direction. Following an additional five-week period and 5,670 patterning cycles, bringing the total number of patterns to 9,828, a third-dimensional inspection was performed. Unlike the second measurement stage, the height dimensions of the GG25 pattern remained nearly unchanged, while significant reductions were observed in the diameter measurements. Specifically, the 38.27 mm diameter decreased by 0.18 mm and the 59 mm diameter by 0.14 mm compared to the previous measurement. A similar trend was observed for the GGG50 pattern, where both diameter dimensions exhibited wear of approximately 0.10 mm, while the height dimensions remained stable. This shift in wear behaviour suggests a change in dominant wear mechanisms with increasing patterning cycles, from axial contact-driven wear to circumferential abrasion and sand induced erosion.

After an additional month of production and 6,966 further patterning cycles, the total number of patterns reached 16,794, and the final measurements were conducted after removing the patterns from the patterning line. At this final stage, dimensional changes in the diameter measurements were negligible, whereas pronounced wear was again observed in the height dimensions. For the GGG50 pattern, the maximum dimensional reduction was measured as 0.18 mm at the 50 mm height, while the minimum change was 0.01 mm at the 59 mm diameter. Similarly, the GG25 pattern exhibited its largest dimensional change at the 50 mm height (0.19 mm), with the smallest change again observed at the 59 mm diameter (0.01 mm). The dimensional tolerance specified for pattern manufacturing was ±0.2 mm. Dimensional measurements in this study were performed using a digital measuring instrument with a resolution of 0.02 mm. Table 4 shows the dimensional differences of the patterns, Table 5 shows the properties of GG25 and GGG50 cast irons, and Table 6 shows the hardness values for GG25 and GGG50 cast irons.

Table 4. Dimensional difference of patterns

Grades	Measurements		
	First (mm)	Last (mm)	Difference (mm)
GG25	38.27	38.05	0.22
	59.06	58.86	0.2
	50.08	49.76	0.32
	9.94	9.82	0.12
GGG50	38.28	38.05	0.23
	59.08	58.84	0.24
	50.07	49.76	0.31
	9.96	9.81	0.15

Table 5. Mass values before and after pattering and surface area values before and after wear of GG25 and GGG50 cast irons

Samples	initial mass (g)	Final mass (g)	absolute mass loss	percentage mass loss	Surface area before wear (mm^2)	Surface area after wear (mm^2)	Normalized Mass Loss (g/mm^2)
GG25	526.92	526.34	0.58	0.11	8160.22	8082.03	7,11e^{-5}
GGG50	516.94	516.12	0.82	0,16	8282.25	8083.7	9,90e^{-5}

Table 6. Hardness values of GG25 and GGG50 cast irons

Materials	Measurement-1 (HB)	Measurement-2 (HB)	Measurement-3 (HB)	Mean ± standard deviation
GG25	212	218	215	215 ± 3
GGG50	218	223	221	221 ± 3

Measurements were taken after each pattering process on GG25 and GGG50 cast irons. These measurements were taken from three different points on the sample surface, and the average of these values was used to calculate the result. Since the results of the measurements taken after each process were very small, only the initial and final measurement values are considered in Table 5. Furthermore, the mounting holes do not affect weight loss because they are drilled at the bottom, where the patterns sit on the plate. The patterns are mounted on the plate and securely fastened from underneath with two Allen-head bolts. Therefore, sand can't accumulate between the pattern and the plate. The only difference is in the depth of the mounting holes, which does not affect the fastening. Since the wear pattern is in the top surface layer, the difference in the number of holes does not affect the wear test.

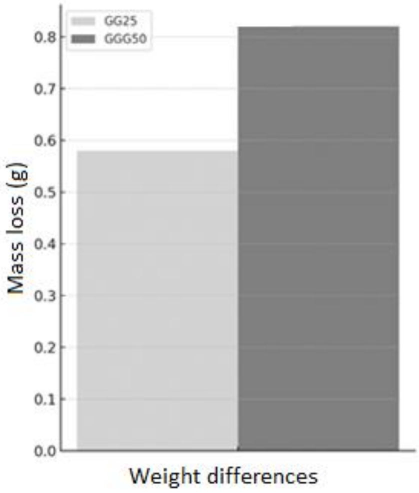

Figure 2. Comparison of the total mass loss of GG25 and GGG50 grade patterns

In parallel, the weight-loss results shown in Figure 2 indicate a greater total mass loss for the GGG50 pattern than for GG25. Figure 3 graphically shows a comparison of millimeter wear between GG25 and GGG50 samples. The millimetric wear trends presented in Table 2 indicate that both materials experienced non-uniform wear depending on geometry and patterning stage. Although GG25 and GGG50 exhibited comparable maximum dimensional reductions at the end of the test period, the progression and distribution of wear differed between the two materials. The observed differences in dimensional wear behavior between GG25 and GGG50 under tested industrial conditions suggest that material-dependent factors may influence wear performance during repetitive green sand pattering processes. However, since direct microstructural characterization was not performed in this study, information regarding the observed dimensional wear behavior is not available.

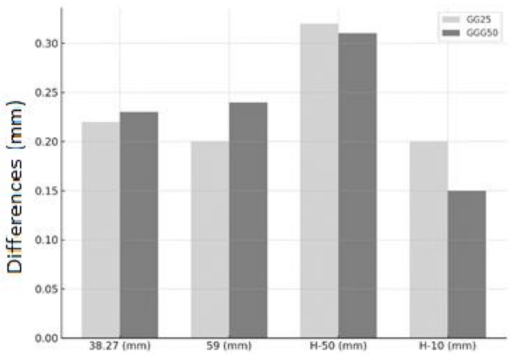

Figure 3. Comparison of final cumulative differences in wear of GG25 and GGG50 samples

Overall, the results show that the dimensional wear behavior of pattern materials in the green sand patterning method is influenced by geometry and potentially material-related factors. Height dimensions, particularly the 50 mm region, were identified as the most critical areas in terms of wear progression. These findings emphasize that pattern preparation should not rely solely on initial surface quality or dimensional accuracy but also consider long-term dimensional wear behavior under actual production conditions.

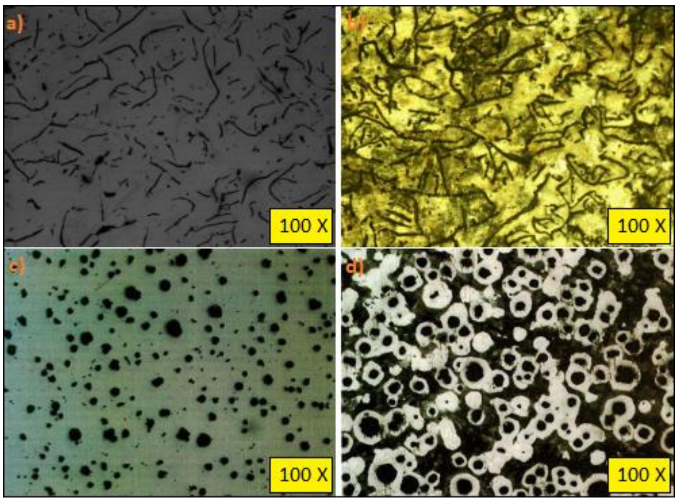

Figure 4. Optical microscope image of GG25 and GGG50 branded cast irons

Figure 4 shows the optical microscope images of GG25 and GGG50 brand cast irons. GG25 and GGG50 cast irons were etched in 2% Nital solution for 15 seconds to reveal the phases within the structure before optical microscopy examination. Figure 4a-b shows the lamellar graphite morphology in the optical microscope image of GG25 gray cast iron. Graphite structures sometimes exhibit a tendency to clump together. The matrix phase is heterogeneous, with lighter areas representing the ferritic phase and thin lamellae in the darker region representing the pearlitic phase. A higher pearlite fraction may reduce ductility relative to ferritic regions; however, further microstructural analysis would be required to confirm this for the tested samples. The results are consistent with the expected microstructure for GG25 gray cast iron. Figure 4c-d shows an optical microscope image of GGG50 spheroidal cast iron. In the image, the dark colors clearly show isolated and densely distributed spherical graphite grains. The graphite grains are round/oval in shape and have slightly irregular contours. Although the grains in GGG50 cast iron show a homogeneous distribution, localized areas of concentration are present.

4. Conclusion

This work investigated the dimensional wear characteristics of GG25 grey cast iron and GGG50 ductile cast iron pattern materials under actual industrial green sand patterning conditions over a total of 16,794 patterning cycles. The evaluation was based on weight loss measurements, dimensional deviations, and the surface finish obtained immediately after machining. Both materials demonstrated comparable dimensional wear throughout the test period, although GG25 showed lower measured mass loss in this single industrial trial; however, this should be interpreted as an observational trend rather than statistically proven superior wear resistance under the applied production conditions. Surface roughness was measured before patterning to characterize the initial machined surface finish. Since roughness measurements were not performed after the patterning cycles, the current results cannot be used to evaluate changes in surface topography or surface quality resulting from exposure to abrasive raw sand during use. The results of this study should also be evaluated in light of several experimental limitations. The use of a single specimen for each material, small variations in pattern geometry, the lack of systematic quantitative monitoring of sand properties, the absence of post-use roughness assessment, and the absence of post-service worn-surface analysis, and local hardness evaluation limits mechanistic interpretation of the underlying abrasion mechanisms. Consequently, the present investigation provides an initial comparison of the dimensional wear performance of GG25 and GGG50 pattern materials under industrial operating conditions together with their initial machined surface characteristics. Further studies employing identical specimen geometries, replicated testing, continuous monitoring of sand properties, post-service surface characterization, and detailed microstructural analyses are required to establish statistically reliable results and to better explain the mechanisms governing material wear.

Declaration of Conflict of Interests

The authors declare that there is no conflict of interest. They have no known competing financial interests or personal relationships that could have appeared to influence the work reported in this paper.

References

[1.] Yalamaç, E., Türkmen, İ. & Fırtına, Ö. Characterization and Kinetic Analysis of Iron Boride Layer Formed on the GGG 70 Ductile Cast Iron. Trans Indian Inst Met 74, 1701–1711 (2021). https://doi.org/10.1007/s12666-021-02249-y.

[2.] Davis, J.R., ASM specialty handbook: cast irons. 1996: ASM international.

[3.] Saeger Jr., Ash, Properties of gray cast iron as affected by casting conditions. 1933. Trans. Am. Foundrymen's Assn, 41: p. 449.

[4.] Landesberger, M., Koos, R., Hofmann, M., Li, X., Boll, T., Petry, W., & Volk, W. (2020). Phase Transition Kinetics in Austempered Ductile Iron (ADI) with Regard to Mo Content. Materials, 13(22), 5266. https://doi.org/10.3390/ma13225266.

[5.] Binali, R., & Kuntoğlu, M. (2023). Evaluation of Machining Parameters Affecting Cutting Forces in Dry Turning of GGG50 Ductile Cast Iron. Turkish Journal of Nature and Science, 12(2), 55-60. https://doi.org/10.46810/tdfd.1210013

[6.] Callister Jr, W.D. and D.G. Rethwisch, Materials science and engineering: an introduction. 2020: John wiley & sons.

[7.] Martin, R., S. Moreno., Effects of different inoculants on the microstructural characteristics of gray cast iron gg-25, hardness and useful life of tools. 2015. 37(4): p. 355-360. Doi: 10.4025/actascitechnol.v37i4.27460

[8.] Del Val, A.G., et al., Wear mechanisms of TiN coated tools during high-speed tapping of GGG50 nodular cast iron. 2023. 514: p. 204558.

[9.] Yıldırım, M., Gümüş, H., & Özcan, M. E. (2025). Investigation of microstructures, mechanical properties, wear behavior and machinability of EN-GJS-500-7 (GGG50) grade ductile cast irons having modified chemical composition. Pamukkale Üniversitesi Mühendislik Bilimleri Dergisi, 31(7), 1143-1149. https://doi.org/10.5505/pajes.2025.79958.

[10.] Holtzer, M., M. Górny, and R. Dańko, Microstructure and properties of ductile iron and compacted graphite iron castings: the effects of mold sand/metal interface phenomena. 2015: Springer. Electronic ISSN:2192-1105

[11.] Wang, B., et al., A review: phase transformation and wear mechanisms of single-step and dual-step austempered ductile irons. Journal of Materials Research and Technology. 2020. 9(1): p. 1054-1069. https://doi.org/10.1016/j.jmrt.2019.10.074

[12.] Seidu, S.O., et al., Effects of additives on some selected properties of base sand. Journal of Minerals and Materials characterization and Engineering. Journal of Minerals and Materials Characterization and Engineering. 2014. 2(5): p. 507-512. http://dx.doi.org/10.4236/jmmce.2014.25051

[13.] Ramkumar, T., et al., Effect of nickel on the microstructure, mechanical and tribological properties of austempered ductile cast iron for steering knuckle applications. Archives of Metallurgy and Materials. 2020. 65(1). DOI: 10.24425/amm.2019.131092

[14.] Elorz, J., F. González, and L.F. Verdeja, Physical metallurgy of cast irons. 2018: Springer. https://doi.org/10.1007/978-3-319-97313-5

[15.] Yakut, R., Investigation of mechanical properties of grey cast irons reinforced with carbon titanium nitride (TiNC). Lubricants. 2023. 11(10): p. 454. https://doi.org/10.3390/lubricants11100454

[16.] Khalifa, D., Mzali F., and A. Science, Study of the effect of green sand properties on thermal conductivity variation of sand mould. Journal of Engineering and Applied Science. 2024. 71(1): p. 178. https://doi.org/10.1186/s44147-024-00493-9

[17.] Gal, B., Nowak, D. Nondestructive, Microwave Testing of Compression Strength and Moisture Content of Green Molding Sands. J Nondestruct Eval 40, 86 (2021). https://doi.org/10.1007/s10921-021-00819-0

[18.] Seidu, S., Effect of compositional changes on the mechanical behaviour of grey cast iron. Journal of Metallurgical Engineering. 2014. 3(2). doi: 10.14355/me.2014.0302.05

[19.] Bramaramba, V., Sen, S. Optimization Study on Sliding Wear Characteristics and Heat-Treatment Conditions of Different Grades of Ferritic Ductile Cast Iron. Trans Indian Inst Met 73, 1131–1146 (2020). https://doi.org/10.1007/s12666-020-01947-3.

How to Cite This Article

Zeynalli, A., and Tekin, D., Comparison of Abrasion Resistance and Surface Roughness of Foundry Patterns Produced from GG25 and GGG50 Grade Cast Iron, Brilliant Engineering, 4(2026), 41143.
https://doi.org/10.36937/ben.2026.41143